Kinetic Study of 2-Propanol and Benzyl Alcohol Oxidation by Alkaline Hexacyanoferrate(III) Catalyzed by a Terpyridyl Ruthenium Complex

ERIC P. KELSON, PROMA P. PHENGSY

Department of Chemistry, California State University at Northridge, Northridge, CA 91330, USA

Received 8 February 2000; accepted 20 June 2000

ABSTRACT: The complex (Trpy)$RuCl_3$ (Trpy = 2,2′:6′,2″-terpyridine) reacts with alkaline hexacyanoferrate(III) to form a terpyridyl ruthenium(IV)-oxo complex that catalyzes the oxidation of 2-propanol and benzyl alcohol by alkaline hexacyanoferrate(III). The reaction kinetics of this catalytic oxidation have been studied photometrically. The reaction rate shows a first-order dependence on [Ru(IV)], a zero-order dependence on [hexacyanoferrate(III)], a fractional order in [substrate], and a fractional inverse order in [HO^-]. The kinetic data suggest a reaction mechanism in which the catalytic species and its protonated form oxidize the uncoordinated alcohol in parallel slow steps. Isotope effects, substituent effects, and product studies suggest that both species oxidize alcohol through similar pericyclic processes. The reduced catalytic intermediates react rapidly with hexacyanoferrate(III) and hydroxide to reform the unprotonated catalytic species. © 2000 John Wiley & Sons, Inc. Int J Chem Kinet 32: 760–770, 2000

INTRODUCTION

Simple oxo-complexes of ruthenium including ruthenate, perruthenate, and ruthenium tetroxide have been extensively studied for their ability to catalyze the oxidation of alcohols by inexpensive co-oxidants [1]. A particularly interesting aspect of this reactivity is the capability to utilize relatively mild co-oxidants such as hexacyanoferrate(III) under alkaline conditions [2–5]. The reported kinetics of ruthenate-catalyzed alcohol oxidation by alkaline hexacyanoferrate(III) suggest that the surprising mild and selective activity of the catalyst comes from the coordination of the alcohol to ruthenium followed by an inner-sphere oxidation of the alcohol [2–5].

Polypyridine donors offer a means of gaining ligand control over high-oxidation-state ruthenium chemistry. Although polypyridine ruthenium complexes are well known for the stoichiometric, catalytic, and electrocatalytic oxidation of alcohols in aqueous and nonaqueous media [6–8], this chemistry has yet to be investigated under alkaline conditions. Polypyridine ligand systems have several advantages. The synthetic chemistry of these systems is well established, which allows ligand variations to be made eas-

Correspondence to: E. P. Kelson (kelson@csun.edu)

ily. Ligand variations have been shown to influence the electrochemical potential of ruthenium-oxo complexes and the specifics of their activity. Polypyridine ruthenium complexes are also notable for their inherent stability, which makes them well suited for kinetic investigations.

We report here the formation of a high-oxidation-state ruthenium-oxo species from (Trpy)$RuCl_3$ (Trpy is 2,2′:6′,2″-terpyridine) and describe the kinetics of its catalytic activity toward alcohol oxidation by hexacyanoferrate(III) in aqueous hydroxide.

EXPERIMENTAL

Materials and Instrumentation

House deionized water was repurified with a Barnstead Super-Q system. Deuterium oxide, 99.8% (Cambridge Isotope Laboratories), potassium hexacyanoferrate(III) (Aldrich), and sodium hydroxide (Fisher Scientific), sodium perchlorate (Alfa-Aesar) were used without additional purification. The complex (Trpy)$RuCl_3$ was prepared as previously reported from the reaction of $RuCl_3 \cdot xH_2O$ (Alfa-Aesar) and Trpy (Aldrich) in ethanol [9]. Dideuteriophenylcarbinol (benzyl alcohol-α,α-d_2), cyclopropyl methanol, and cyclobutanol were obtained from Aldrich and used without further purification. All other substrates were obtained from the Aldrich Chemical Co. and purified by vacuum distillation or recrystallization. Purities were verified by GC-FID. All other materials were reagent grade and were used without additional purification.

UV-visible spectra were recorded on a Hewlett Packard 8452 diode array spectrophotometer with a Peltier thermostatted cell holder. GC-FID analyses were carried out with a Hewlett Packard 5890 Series II gas chromatograph with a HP-Wax column (30 m length, 0.32-mm diameter, 0.25-μm film thickness). Global Factor Analysis of spectra was performed with SPECFIT/32 (Spectrum Software Associates) running in Windows 95. Further kinetic analyses were carried out in Kaleidagraph 3.0 (Abelbeck Software) in Macintosh OS 8.5.

Products and Stoichiometry

Products and yields from the oxidation of benzyl, 4-methoxybenzyl, and 4-nitrobenzyl alcohols were measured as follows. The precatalyst (Trpy)$RuCl_3$ (2.6 mg, 5.9 μmol) was added to 10.0 mL of 0.30 M NaOH and dissolved by stirring in a 45°C water bath for 5 min. Then 10.0 mL of 12.0 mM $K_3Fe(CN)_6$ was added, and the solution was stirred in a 35°C water bath for 30 minutes to complete formation of the catalytic species. The resulting solution was then diluted with 30.0 mL of water, and additional $K_3Fe(CN)_6$ (0.388 g, 1.18 mmol) was added and dissolved. Then 10.0 mL of the catalyst/oxidant solution and 10 mL of the substrate solution (see Table I) were thermally equilibrated at 25°C and mixed. After 30 min, the reaction was carefully acidified with 0.30 M HCl and extracted three times with 10 mL portions of CH_2Cl_2. The extracts were dried with Na_2SO_4 and analyzed by GC-FID. The benzyl alcohols and the corresponding benzaldehyde and benzoic acid products (Table I) were identified by their retention times.

Products from the oxidation of cyclopropyl methanol and cyclobutanol were determined as follows. The precatalyst (Trpy)$RuCl_3$ (2.6 mg, 5.9 μmol) was added to 1.00 mL of 0.30 M NaOH and dissolved by stirring in a 45°C water bath for 10 minutes. Then 3.00 mL of water and 1.00 mL of 0.156 M $K_3Fe(CN)_6$ were sequentially added to the catalyst solution, and the catalyst/oxidant solution was stirred in a 35°C water bath for 30 min. Then 30 μL of the substrate (cyclopropyl methanol or cyclobutanol) was added, and the reaction was stirred in a 35°C bath. On completion of the reaction (within 5 min), the solution was carefully acidified with 0.30 M $HClO_4$, and the resulting solution

Table I Oxidation of Benzyl Alcohols by the (Trpy)$RuCl_3$/$Fe(CN)_6^{3-}$/HO^- System after 30 Min at 25°C[a]

Substrate	$[ROH]_0/[Fe^{III}]_0$	Product	Turnovers	% Yield
Benzyl alcohol	1.0	Benzaldehyde	101	93
Benzyl alcohol	0.5	Benzaldehyde	92	84
		Benzoic acid	6	6
4-Methoxybenzyl alcohol	1.0	4-Methoxybenzaldehyde	103	95
4-Nitrobenzyl alcohol	1.0	4-Nitrobenzaldehyde	37	34
		4-Nitrobenzoic acid	62	57

[a] Reactions carried out in water with $[Ru]_T = 5.9 \cdot 10^{-5}$ M; $[K_3Fe(CN)_6^{3-}] = 1.28 \cdot 10^{-2}$ M; $[NaOH] = 3.0 \cdot 10^{-2}$ M. Yields based on amount of oxidant consumed. Turnovers based on stoichiometries in Eqs. (1) and (2) in which benzoic acids are formed sequentially through benzaldehyde through two turnovers of catalyst.

was analyzed by GC-FID directly. The carbonyl products (cyclopropanecarbaldehyde and cyclobutanone) were confirmed by their retention times.

The oxidation of triphenylphosphine was confirmed and quantified as follows. The precatalyst (Trpy)$RuCl_3$ (2.0 mg, 4.5 μmol) was added to 2.0 mL of 0.172 M NaOH and dissolved by stirring in a 45°C water bath for 5 min. Then 50 mL of 0.172 M NaOH and 50 mL of 4.3 mM $K_3Fe(CN)_6$ were sequentially added to the catalyst solution, and the catalyst/oxidant solution was stirred in a 35°C water bath for 30 min. Then freshly ground PPh_3 (0.137 g, 0.52 mmol) was added, and the reaction was stirred vigorously in a 45°C oil bath until the yellow color of $Fe(CN)_6^{3-}$ disappeared. Then a 3.0-mL portion of the resulting suspension was extracted with 1.0 mL of CH_2Cl_2, and the extract was analyzed by GC-FID. Triphenylphosphine oxide product and unreacted triphenylphosphine were identified by their retention times and quantified through FID integrations.

The dissociation of chloride ligands from (Trpy)$RuCl_3$ in NaOH was quantified as follows. The complex (Trpy)$RuCl_3$ (0.100 g, 0.23 mmol) was added to 38 mL of 0.30 M NaOH and dissolved by stirring in a 45°C water bath for 10 min. The reaction was quickly acidified with 1.0 M $HClO_4$ and treated with 2.0 mL of 0.57 M $AgNO_3$ (1.14 mmol). The resulting AgCl was immediately isolated by centrifugation, washed, and dried *in vacuo.* This afforded 0.0923 g of AgCl, which corresponds to a 95% yield, assuming all three chlorides of (Trpy)$RuCl_3$ dissociate.

Kinetic Measurements

Rate data for the consumption of the oxidant $Fe(CN)_6^{3-}$ were collected by following absorbance decreases in its λ_{max} at 420 nm. Besides the decay of this peak, no other changes occur in the reaction spectra until the $Fe(CN)_6^{3-}$ is almost completely consumed. Further, the decay of 420 nm vs. time is linear for most of the reaction. For these reasons, initial reaction rates were calculated through the relation $\nu_{obs} = -\delta[Fe(CN)_6^{3-}]/\delta t = -(\delta A_{420}/\delta t)/(\varepsilon_{III} - \varepsilon_{II})b$ in which $\delta A_{420}/\delta t$ was the least-squares slope for the absorbance decay at 420 nm, ε_{III} and ε_{II} were the absorptivities of $Fe(CN)_6^{3-}$ and $Fe(CN)_6^{4-}$ at 420 nm (measured as $1.04 \cdot 10^3$ $M^{-1}cm^{-1}$, and 1.41 $M^{-1}cm^{-1}$, respectively), and b was the cell path length (1.00 cm).

A typical kinetic run was initiated by the addition of 0.50 mL of alcohol solution to 2.5 mL of solution containing the catalyst, $K_3Fe(CN)_6$, NaOH, and $NaClO_4$. The alcohol solutions were prepared volumetrically to provide typical reaction concentrations of $2.0 \cdot 10^{-2}$ M of aliphatic alcohols or $6.7 \cdot 10^{-4}$ M of benzyl alcohols. The catalyst/oxidant/hydroxide solution was prepared by the combination of stock solutions to give typical reaction concentrations of 0.100 mM catalyst, 1.7 mM $Fe(CN)_6^{3-}$, and 50 mM OH^-. The ionic strength of each reaction was adjusted to $\mu = 0.50$ M by the appropriate amount of $NaClO_4$. To ensure the reproducible formation of the catalytic species from (Trpy)$RuCl_3$, the catalyst solution was prepared as follows. The precatalyst (Trpy)$RuCl_3$ (2.6 mg, 5.9 μmol) was added to 10.0 mL of 0.30 M NaOH and stirred in a 45°C water bath for 5 min. Then 10.0 mL of 12 mM $K_3Fe(CN)_6$ was added, and the solution was stirred in a 35°C water bath for 30 min. During this time, three equivalents of $Fe(CN)_6^{3-}$ are consumed by the ruthenium complex to form the catalytic intermediate. This procedure gives a solution that is 0.30 mM in catalyst, 5.1 mM in $Fe(CN)_6^{3-}$, and 0.15 M in OH^-.

Purging reaction solutions with argon had no apparent effect on reaction kinetics, so reactions were not deoxygenated.

RESULTS

Stoichiometry and Products

As shown in Table I, the precatalyst (Trpy)$RuCl_3$ in alkaline hexacyanoferrate(III) effectively oxidizes benzyl alcohols to benzaldehyde and acid products. Oxidation of excess benzyl and 4-methoxybenzyl alcohols exclusively produces the corresponding aldehydes according to the stoichiometry in Eq. (1).

$$C_6H_5CH_2OH + 2Fe(CN)_6^{3-} + 2OH^- \longrightarrow C_6H_5CHO + 2Fe(CN)_6^{4-} + 2H_2O \quad (1)$$

Stoichiometric oxidation of benzyl alcohol affords a small yield of benzoic acid that is likely formed from oxidation of product benzaldehyde according to the stoichiometry in Eq. (2).

$$C_6H_5CHO + 2Fe(CN)_6^{3-} + 2OH^- \longrightarrow C_6H_5CO_2H + 2Fe(CN)_6^{4-} + 2H_2O \quad (2)$$

The oxidation of twice the stoichiometric amount of 4-nitrobenzyl alcohol affords a significant amount of the benzoic acid, indicating the electron-withdrawing nitro group encourages benzaldehyde oxidation. Electron-withdrawing groups have also been reported to accelerate the oxidation of substituted benzaldehydes [10] and furfurals [11] by alkaline permanganate. The electron-withdrawing substituent may be encouraging the reaction of 4-nitrobenzaldehyde with hydroxide to

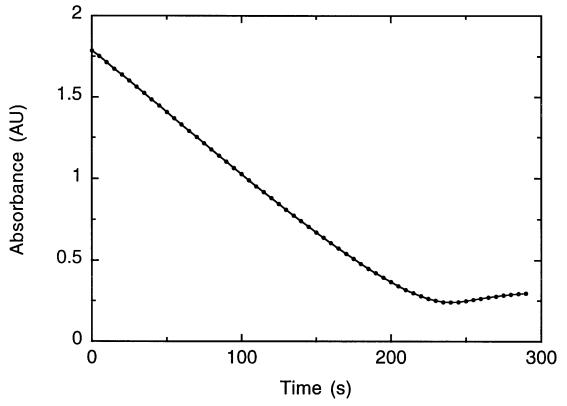

Figure 1 Absorbance trace (420 nm) vs. time plot for the oxidation of 2-propanol catalyzed by the (Trpy)$RuCl_3$/$Fe(CN)_6^{3-}$/HO^- system in water, [2-propanol] = $5.2 \cdot 10^{-2}$ M, $[Ru]_T = 1.00 \cdot 10^{-4}$ M, $[K_3Fe(CN)_6] = 1.7 \cdot 10^{-3}$ M, [NaOH] = $5.0 \cdot 10^{-2}$ M, $[NaClO_4]$ = 0.45 M at 35°C.

form the $4\text{-}NO_2C_6H_4CH(OH)(O)^-$ anion. Rapid oxidation of this electron- rich intermediate would produce the observed benzoic acid. The mechanism of aldehyde oxidation by this catalytic system is under investigation.

Spectral Changes

The precatalyst **1** dissolves into alkaline hexacyanoferrate(III) to form a complex with a λ_{max} at 472 nm ($\varepsilon = 1.8 \cdot 10^3\ M^{-1}cm^{-1}$). The addition of alcohol to a solution of (Trpy)$RuCl_3$ in alkaline hexacyanoferrate(III) results in the decay of the λ_{max} of hexacyanoferrate(III) at 420 nm. In the early stages of the catalytic reaction, no other changes occur in the spectrum. The peak at 472 nm disappears shortly after depletion of hexacyanoferrate(III) and reappears upon the addition of more oxidant. This peak at 472 nm likely represents the oxidized form of the catalyst that predominates in the presence of oxidant. Since the initial spectral changes during catalytic reactions appear to be only the consumption of hexacyanoferrate(III), the early progress of the reaction was easily monitored through the decay in the absorption at 420 nm.

Kinetics

Effect of $Fe(CN)_6^{3-}$ Concentration. When an excess of hexacyanoferrate(III) is present with respect to ruthenium, the decay of the 420 nm absorbance of hexacyanoferrate(III) is linear, indicating a zero-order dependence on the oxidant (Fig. 1). This linearity was unaffected by reaction conditions used in this study. This made measurement of initial reaction rates straightforward from the initial slope of absorption versus time data. Typical initial reaction rates are listed in Table II.

Effect of Catalyst Concentration. Plots of ν_{obs} vs. catalyst concentration are linear with zero-intercepts (Fig. 2) over the concentrations used in this study. This confirms that the reaction is first order to catalyst concentration and the rate of the uncatalyzed reaction is negligible compared to the catalyzed oxidation.

Effect of Substrate Concentration. At low concentrations of 2-propanol and benzyl alcohol, the initial rates are proportional to [alcohol]; at higher concentrations of both alcohols saturation-type kinetics are observed. Plots of $1/\nu_{obs}$ vs. 1/[alcohol] for 2-propanol (Fig. 3) and benzyl alcohol (Fig. 4) are linear with positive slopes and small intercepts, consistent with Eq. (3).

Table II Representative Zero-Order Rate Constants for Alcohol Oxidation by the (Trpy)$RuCl_3$/$Fe(CN)_6^{3-}$/HO^- System[a]

Substrate	[Substrate] (M)	ν_{obs} (10^{-6} M · s^{-1})
2-Propyl alcohol	$2.0 \cdot 10^{-2}$	4.4
2-Propyl alcohol-d_8	$2.0 \cdot 10^{-2}$	0.89
Benzyl alcohol	$6.7 \cdot 10^{-4}$	3.38
Benzyl-α,α-d_2 alcohol	$6.7 \cdot 10^{-4}$	0.80
4-Methoxybenzyl alcohol	$6.7 \cdot 10^{-4}$	3.52
4-Methylbenzyl alcohol	$6.7 \cdot 10^{-4}$	3.45
4-Fluorobenzyl alcohol	$6.7 \cdot 10^{-4}$	3.06
4-Chlorobenzyl alcohol	$6.7 \cdot 10^{-4}$	3.69
4-Trifluoromethylbenzyl alcohol	$6.7 \cdot 10^{-4}$	4.02
4-Nitrobenzyl alcohol	$6.7 \cdot 10^{-4}$	6.29

[a] Reactions carried out in water with $[Ru]_T = 1.0 \cdot 10^{-4}$ M; $[K_3Fe(CN)_6] = 1.7 \cdot 10^{-3}$ M; [NaOH] = $5.0 \cdot 10^{-2}$ M; $[NaClO_4]$ = 0.45 M at 25°C for benzyl alcohols and 35°C for 2-propyl alcohols.

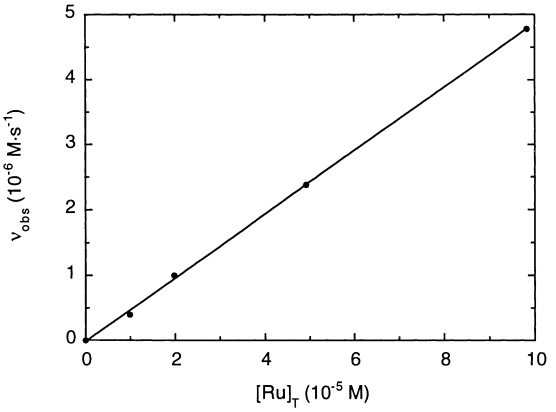

Figure 2 Plot of ν_{obs} vs. $[Ru]_T$ for 2-propanol oxidation catalyzed by the (Trpy)$RuCl_3$/$Fe(CN)_6^{3-}$/HO^- system in water, $[K_3Fe(CN)_6] = 1.7 \cdot 10^{-3}$ M, [2-propanol] = $2.2 \cdot 10^{-2}$ M, [NaOH] = $5.0 \cdot 10^{-2}$ M, $[NaClO_4]$ = 0.45 M at 35°C.

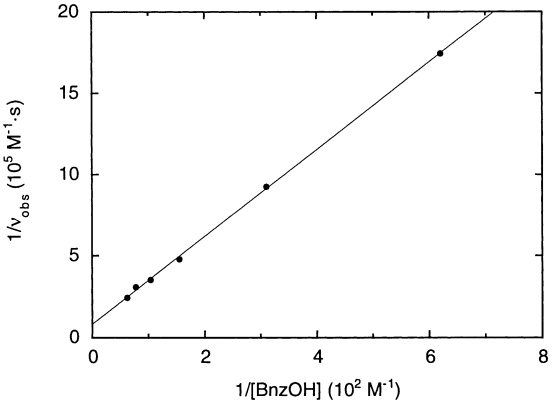

Figure 4 Plot of $1/\nu_{obs}$ vs. 1/[BnzOH] for benzyl alcohol oxidation catalyzed by the (Trpy)$RuCl_3$/$Fe(CN)_6^{3-}$/HO^- system in water, $[Ru]_T = 1.6 \cdot 10^{-5}$ M, $[K_3Fe(CN)_6] = 2.0 \cdot 10^{-3}$ M, [NaOH] = $5.0 \cdot 10^{-2}$ M, $[NaClO_4]$ = 0.45 M at 25°C.

$$\frac{1}{\nu_{obs}} = a_1 + \frac{a_2}{[\text{alcohol}]} \qquad (3)$$

Although this suggests alcohol coordination is involved in the reaction mechanism, the initial rates for 2-propanol oxidation are not affected by large concentrations of added *tert*-butanol (up to 0.2 M). High concentrations of 2-propanol also do not change the 472 nm peak in the reaction spectra in any noticeable way.

Effect of Hydroxide Concentration. The initial rates for the oxidation of 2-propanol and benzyl alcohol increase with decreasing concentrations of hydroxide. The plot of ν_{obs} vs. 1/[HO^-] for 2-propanol (Fig. 5) is linear with a positive slope and a small intercept consistent with Eq. (4).

$$\nu_{obs} = b_1 + \frac{b_2}{[HO^-]} = \frac{b_1[HO^-] + b_2}{[HO^-]} \qquad (4)$$

The plot of ν_{obs} vs. 1/[HO^-] for benzyl alcohol (Fig. 6) was not linear, but a plot of ν_{obs} vs. 1/[HO^-] was easily fit to Eq. (5).

$$\nu_{obs} = \frac{c_1(1/[HO^-]) + c_2}{c_3(1/[HO^-]) + 1} = \frac{c_1 + c_2[HO^-]}{c_3 + [HO^-]} \qquad (5)$$

Although reaction rates were very fast at low hydrox-

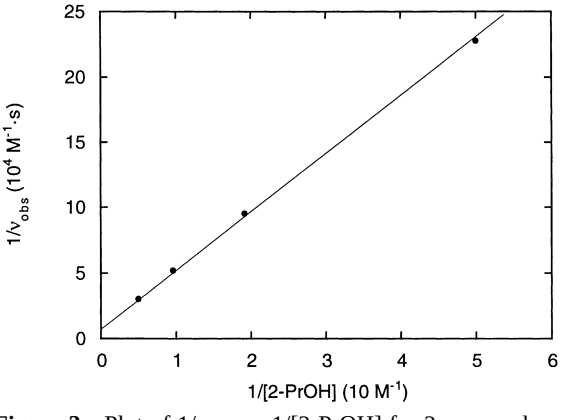

Figure 3 Plot of $1/\nu_{obs}$ vs. 1/[2-PrOH] for 2-propanol oxidation catalyzed by the (Trpy)$RuCl_3$/$Fe(CN)_6^{3-}$/HO^- system in water, $[Ru]_T = 1.0 \cdot 10^{-4}$ M, $[K_3Fe(CN)_6] = 1.7 \cdot 10^{-3}$ M, [NaOH] = $5.0 \cdot 10^{-2}$ M, $[NaClO_4]$ = 0.45 M at 35°C.

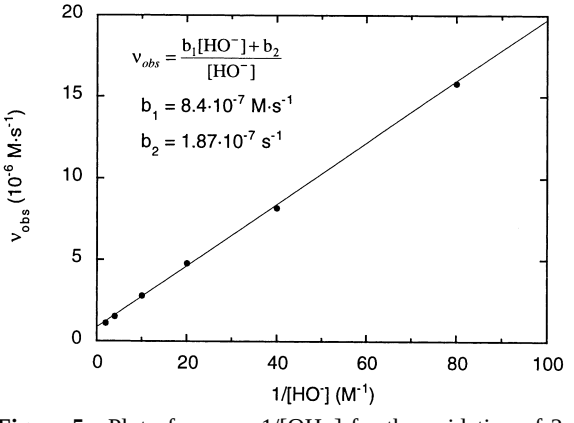

Figure 5 Plot of ν_{obs} vs. 1/[OH^-] for the oxidation of 2-propanol catalyzed by the (Trpy)$RuCl_3$/$Fe(CN)_6^{3-}$/HO^- system in water, $[Ru]_T = 1.0 \cdot 10^{-4}$ M, $[K_3Fe(CN)_6] = 1.7 \cdot 10^{-3}$ M, [2-propanol] = $2.2 \cdot 10^{-2}$ M, μ = 0.50 M at 35°C. ($NaClO_4$ added to adjust ionic strength to 0.50 M.)

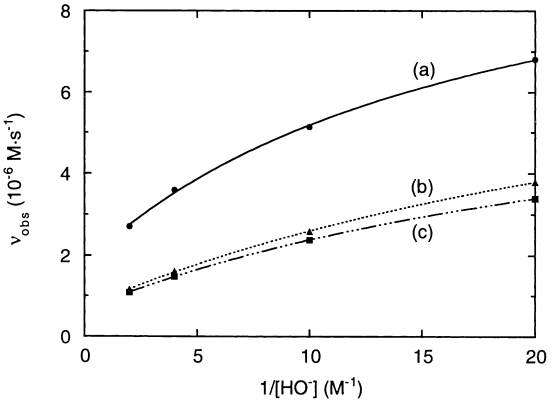

Figure 6 Plot of ν_{obs} vs. 1/[OH^-] for the oxidation of (a) 4-$NO_2C_6H_4CH_2OH$, (b) 4-$CH_3OC_6H_4CH_2OH$, and (c) $C_6H_5CH_2OH$ catalyzed by the (Trpy)$RuCl_3$/$Fe(CN)_6^{3-}$/HO^- system in water, $[Ru]_T = 1.00 \cdot 10^{-4}$ M, $[K_3Fe(CN)_6] = 1.7 \cdot 10^{-3}$ M, [Alc.] $= 6.7 \cdot 10^{-4}$ M, $\mu = 0.50$ M at 25°C. ($NaClO_4$ added to adjust ionic strength to 0.50 M.)

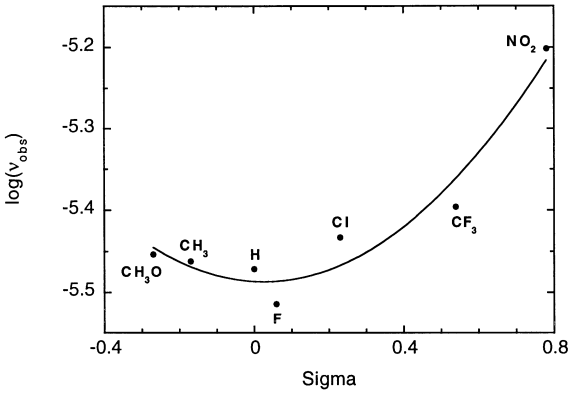

Figure 7 Plot of log(ν_{obs}) vs. Hammett sigma for the oxidation of 4-substituted benzyl alcohols by the (Trpy)$RuCl_3$/$Fe(CN)_6^{3-}$/HO^- system in water, $[Ru]_T = 1.00 \cdot 10^{-4}$ M, $[K_3Fe(CN)_6] = 1.7 \cdot 10^{-3}$ M, $[HO^-] = 5.0 \cdot 10^{-2}$ M, $[NaClO_4] = 0.45$ M at 25°C.

ide concentrations, catalyst turnover numbers rapidly fell below 10 at pH $<$ 11.7. For this reason, kinetic measurements were typically made at pH = 12.7, where turnover numbers were sufficient to fully consume the alcohol many times.

Kinetic Isotope Effects. Primary kinetic isotope effects were observed in the oxidation of 2-propanol ($\nu_{obs,H}/\nu_{obs,D} = 4.9$) at 35°C and benzyl alcohol ($\nu_{obs,H}/\nu_{obs,D} = 4.2$) at 25°C. Significant solvent isotope effects were also observed when the oxidation rates of 4-nitrobenzyl alcohol and 4-methoxybenzyl alcohol in D_2O were compared to those in H_2O ($\nu_{obs,\ H_2O}/\nu_{obs,\ D_2O} = 1.88$ and 1.63, respectively; Table III).

Substituent Effects. An attempted Hammett plot of the initial oxidation rates for 4-substituted benzyl alcohols exhibited a surprising concave curve with its minimum near $\sigma = 0$ (Fig. 7). Both electron-withdrawing and electron-releasing substituents accelerated the reaction, although the effect was stronger for electron-withdrawing groups. Initial rates for the oxidation of 4-nitrobenzyl and 4-methoxybenzyl alcohols exhibited the same dependencies on hexacyanoferrate(III), alcohol, and hydroxide concentrations, as observed for benzyl alcohol.

Free Radical Detection. Free radicals are probable intermediates from the one-electron oxidation of alcohols. The oxidation of radical-clock substrates cyclopropyl methanol and cyclobutanol exclusively formed cyclopropanecarbaldehyde and cyclobutanone, respectively. The lack of ring-opened products indicated that free-radical intermediates were not formed in the oxidation of these substrates [12,13]. Further, deoxygenation of 2-propanol and benzyl alcohol oxidations had no effect on their initial rates. These observations indicate that free radicals are not formed in these reactions.

DISCUSSION

Although attempts at direct isolation of the catalytic complex resulted only in decomposition products, in-

Table III Solvent Kinetic Isotope Effects for Alcohol Oxidation by (Trpy)$RuCl_3$/$Fe(CN)_6^{3-}$/OH^- at 25°C[a]

Substrate	Media	ν_{obs} (10^{-6} M^{-1} s^{-1})	ν_H/ν_D
4-Methoxybenzyl alcohol	H_2O	3.77	1.63
4-Methoxybenzyl alcohol	D_2O	2.31	
4-Nitrobenzyl alcohol	H_2O	8.08	1.88
4-Nitrobenzyl alcohol	D_2O	4.29	

[a] Reactions carried out with $[Ru]_T = 1.40 \cdot 10^{-4}$ M; [Alc.] $= 6.7 \cdot 10^{-4}$M; $[K_3Fe(CN)_6] = 2.5 \cdot 10^{-3}$ M; $[NaOH] = 7.1 \cdot 10^{-2}$ M; $[NaClO_4] = 0.64$ M.

direct evidence suggests that a ruthenium-oxo species is responsible for this reactivity [14]. When a solution of (Trpy)$RuCl_3$ in NaOH is acidified and treated with an excess of silver nitrate, AgCl precipitates immediately in sufficient quantity to account for all three chloride ligands of the precatalyst. This suggests that (Trpy)$RuCl_3$ likely exchanges one or more chloride ligands in NaOH for hydroxide or water. In the spectrophotometric titration of (Trpy)$RuCl_3$ dissolved in NaOH with hexacyanoferrate(III), three equivalents of the oxidant are required to produce the catalytic species (λ_{max} = 472 nm). An excess of hexacyanoferrate(III) results in no further changes. Although the reactions leading to the catalytic species appear complex, the addition of hexacyanoferrate(III) results in an immediate change in the initial spectrum of (Trpy)$RuCl_3$ in NaOH followed by a slow formation of the catalytic species (λ_{max} = 472 nm) over minutes. Since polypyridyl Ru^{IV} complexes such as $[(Bpy)_2(Py)Ru^{IV}(O)]^{2+}$ (where Bpy is 2,2′-bipyridine) and $[(Trpy)(Phen)Ru^{IV}(O)]^{2+}$ are prone to ligand hydroxylation in basic solutions [15], the slower reaction is likely the hydroxylation of the terpyridine ligand in a Ru^{IV} complex. A rapid two-electron oxidation of the resulting Ru^{II} complex would afford a (TrpyO)Ru^{IV}(L)(L′)(L″) complex where $(TrpyO)^-$ is the hydroxylated (and deprotonated) terpyridine ligand and L, L′, L″ are oxo, hydroxyl, aquo, and/or chloro ligands. The oxidation chemistry of $(Bpy)_2Ru^{II}(OH_2)_2^{2+}$ and $(Trpy)Ru^{II}(OH_2)_3^{3+}$ suggests that the high oxidation state of the catalytic species will likely encourage one or more of its ligands to be oxo groups [16,17]. Since reported dimeric and trimeric polypyridine ruthenium complexes all exhibit strong absorption peaks at 600 nm and longer [18], the 472 nm absorption of the catalytic species seems characteristic of a monomer. In addition to catalyzing alcohol oxidation, the catalytic species mediates the oxidation of triphenylphosphine by hexacyanoferrate(III) to form triphenylphosphine oxide. Such oxygen transfer is familiar in metal-oxo chemistry and is consistent with the catalyst being a ruthenium-oxo complex [19–22]. The kinetic isotope effects for both 2-propanol and benzyl alcohol are also typical for alcohol oxidation reactions by ruthenium-oxo systems [23,24]. Overall, a possible formulation for the catalytic species is (TrpyO)Ru^{IV}(O)(L′)(L″) where L′ and L″ are oxo, hydroxyl, aquo, and/or chloro ligands. Attempts to directly prepare and characterize such complexes are underway.

Traditionally, the inverse hydroxide dependence and saturation-like kinetics for alcohols would suggest the exchange of a hydroxyl ligand on the catalytic complex for alcohol. However, terpyridine ruthenium systems are six-coordinate and exchange ligands relatively slowly by dissociative processes. Hydroxide dissociation will not likely be fast enough to account for the observed reaction rates. Further, the presence of *tert*-butanol has no measurable effect on the oxidation rate of 2-propanol even up to a molar ratio of 10 : 1. This is not consistent with an alcohol coordination mechanism, although the steric bulk of *tert*-butanol may attenuate its impact on such a reaction.

The observed inverse hydroxide dependence is more likely a result of proton transfer from water to the predominant form of the catalytic complex, as shown in Eq. (6). An oxo or hydroxyl group likely acts as the proton acceptor.

$$(Ru^{IV}) + H_2O \underset{k_{-1}}{\overset{k_1}{\rightleftharpoons}} H(Ru^{IV})^+ + HO^- \qquad (6)$$

where (Ru^{IV}) = (TrpyO)Ru^{IV}(O)(L′)(L″) and $H(Ru^{IV})^+$ = (TrpyO)Ru^{IV}(O)(HL′)$(L'')^+$. Terpyridine ruthenium-oxo/hydroxyl complexes are noted to have multiple protonation states [16,17], and protonation would enhance the electrophilicity and reactivity of the ruthenium center. Interestingly, proton transfer to and from ruthenium-oxo/hydroxyl complexes can be relatively slow due to accompanying isomerization of the complex. Slow proton transfer and isomerization has been reported in the oxidation of diphosphines by *trans*-$[(Trpy)Ru^{VI}(O)_2(H_2O)]^{2+}$ in water/acetonitrile [25].

The saturation-like kinetics for alcohol concentrations could be due to a slow alcohol oxidation following a relatively sluggish preequilibrium. The simplest mechanism would have this oxidation following the slow protonation step mentioned earlier. This is consistent with the expectation that protonation would produce a more reactive oxidizer for alcohol. The absence of ring-opened products from the oxidation of radical clock substrates and the insensitivity of the reaction to oxygen indicate that the oxidation step does not proceed by hydrogen transfer from the alcohol to form radical intermediates. Alcohol oxidation by the protonated intermediate is more likely a two-electron process to produce a Ru^{II} intermediate, as shown in Eq. (7). The specifics of this reaction will be addressed later in this discussion.

$$H(Ru^{IV})^+ + RR'CHOH \xrightarrow{k_2} H_3(Ru^{II})^+ + RR'C{=}O \qquad (7)$$

where $H_3(Ru^{II})^+$ = (TrpyO)Ru^{II}(OH)$(H_2L')(L'')^+$.

The small intercept in the ν_{obs} vs. 1/[OH^-] plot for the oxidation of 2-propanol (Fig. 5) suggests a parallel alcohol oxidation step independent of the protonation equilibrium. The simplest explanation would have the unprotonated ruthenium species oxidize alcohol as shown in Eq. (8) at a slower rate than the protonated intermediate.

$$(Ru^{IV}) + RR'CHOH \xrightarrow{k_3} H_2(Ru^{II}) + RR'C{=}O \quad (8)$$

where $H_2(Ru^{II})$ = (TrpyO)Ru^{II}(OH)(HL′)(L″).

The zero-order dependence on hexacyanoferrate(III) is consistent with the reduced ruthenium species from alcohol oxidation rapidly reacting with two equivalents of hexacyanoferrate(III) and an appropriate amount of hydroxide to reform the predominant catalytic complex as shown in Eqs. (9) and (10). This would close the catalytic cycle.

$$H_2(Ru^{II}) + 2\ Fe(CN)_6^{3-} + 2\ HO^- \xrightarrow{\text{fast}} (Ru^{IV}) + 2\ Fe(CN)_6^{4-} + 2\ H_2O \quad (9)$$

$$H_3(Ru^{II})^+ + 2\ Fe(CN)_6^{3-} + 3\ HO^- \xrightarrow{\text{fast}} (Ru^{IV}) + 2\ Fe(CN)_6^{4-} + 3\ H_2O \quad (10)$$

Given the hypothetical mechanism outlined in Eqs. (6)–(10), the rate for hexacyanoferrate(III) consumption would be given by Eq. (11):

$$\nu_{obs} = -\frac{d[Fe(CN)_6^{3-}]}{dt} = 2k_2[H(Ru^{IV})^+][ROH] + 2k_3[(Ru^{IV})][ROH] \quad (11)$$

By applying the steady-state hypothesis for [$H(Ru^{IV})^+$], we obtain Eq. (12)

$$[H(Ru^{IV})^+] = \frac{k_1[(Ru^{IV})]}{k_{-1}[HO^-] + k_2[ROH]} \quad (12)$$

Since both $H_2(Ru^{II})$ and $H_3(Ru^{II})^+$ are consumed in fast steps, the amount of both should be negligible as long as hexacyanoferrate(III) is present. The total ruthenium concentration may be given as Eq. (13):

$$[Ru]_T = [(Ru^{IV})] + [H(Ru^{IV})^+] \quad (13)$$

Replacing the expression for [(Ru^{IV})] in terms of [$H(Ru^{IV})^+$] from Eq. (12) into Eq. (13) and then solving for [$H(Ru^{IV})^+$] gives Eq. (14):

$$[H(Ru^{IV})^+] = \frac{k_1}{k_1 + k_{-1}[HO^-] + k_2[ROH]}[Ru]_T \quad (14)$$

Substitution of Eq. (14) into Eq. (13) and then solving for [(Ru^{IV})] leads to Eq. (15):

$$[(Ru^{IV})] = \frac{k_{-1}[HO^-] + k_2[ROH]}{k_1 + k_{-1}[HO^-] + k_2[ROH]}[Ru]_T \quad (15)$$

Substitution of the expressions for [(Ru^{IV})] and [$H(Ru^{IV})^+$], Eqs. (14) and (15), into Eq. (11) leads to Eq. (16):

$$\nu_{obs} = -\frac{d[Fe(CN)_6^{3-}]}{dt} = \frac{2k_1k_2[ROH] + 2k_{-1}k_3[HO^-][ROH] + 2k_2k_3[ROH]^2}{k_1 + k_{-1}[HO^-] + k_2[ROH]}[Ru]_T \quad (16)$$

Since k_2[ROH] and k_3[ROH] represent the slow steps of the catalytic reaction, their product, k_2k_3[ROH]^2, is likely very small compared to k_1k_2[ROH] and $k_{-1}k_3$[HO^-][ROH], so Eq. (16) can be approximated as Eq. (17):

$$\nu_{obs} = -\frac{d[Fe(CN)_6^{3-}]}{dt} \approx \frac{2k_1k_2[ROH] + 2k_{-1}k_3[HO^-][ROH]}{k_1 + k_{-1}[HO^-] + k_2[ROH]}[Ru]_T \quad (17)$$

This rate law is in good agreement with the experimental data. The alcohol dependence in this equation fits the observed relationship in Eq. (3) with the following expressions for a_1 and a_2:

$$a_1 = \frac{k_2}{2(k_{-1}k_3[HO^-] + k_1k_2)[Ru]_T} \quad (18)$$

$$a_2 = \frac{k_1 + k_{-1}[HO^-]}{2(k_{-1}k_3[HO^-] + k_1k_2)[Ru]_T} \quad (19)$$

The rate law in Eq. (17) is also consistent with the hydroxide dependencies for 2-propanol and benzyl alcohol. In the case of 2-propanol, the following ex-

pressions for b_1 and b_2 and the assumption in Eq. (22) make Eq. (17) fit the observed behavior in Eq. (4):

$$b_1 = \frac{2k_{-1}k_3[\mathrm{ROH}][\mathrm{Ru}]_T}{k_{-1}} = 2k_3[\mathrm{ROH}][\mathrm{Ru}]_T \quad (20)$$

$$b_2 = \frac{2k_1k_2[\mathrm{ROH}][\mathrm{Ru}]_T}{k_{-1}} \quad (21)$$

and

$$k_1 + k_2[\mathrm{ROH}] \ll k_{-1}[\mathrm{HO}^-] \quad (22)$$

A relatively small $k_2[\mathrm{ROH}]$ with respect to $k_{-1}[\mathrm{HO}^-]$ is reasonable considering the relatively slow oxidation rates for 2-propanol compared to benzyl alcohol. A small k_1 with respect to $k_{-1}[\mathrm{HO}^-]$ would make the unprotonated species the strongly preferred form of the catalyst over the range of hydroxide concentrations studied. This is consistent with the λ_{max} 472 nm peak (that likely represents the unprotonated catalyst) appearing unchanged by the hydroxide concentration. The relatively small size of k_1 allows Eq. (17) to be simplified to Eq. (23):

$$\nu_{obs} = -\frac{d[\mathrm{Fe(CN)_6}^{3-}]}{dt} \approx \frac{2k_1k_2[\mathrm{ROH}] + 2k_{-1}k_3[\mathrm{HO}^-][\mathrm{ROH}]}{k_{-1}[\mathrm{HO}^-] + k_{-2}[\mathrm{ROH}]}[\mathrm{Ru}]_T \quad (23)$$

The intercept and slope from the plot of ν_{obs} vs. $1/[\mathrm{HO}^-]$ for 2-propanol (Fig. 5) give values of $k_3 = 1.91 \cdot 10^{-1}$ $\mathrm{M^{-1}s^{-1}}$ and $k_1k_2/k_{-1} = 4.25 \cdot 10^{-2}$ $\mathrm{s^{-1}}$ through Eqs. (20) and (21). The contribution of alcohol oxidation by unprotonated catalyst, $(\mathrm{Ru^{IV}})$ to the observed rate, ν_{obs}, can be calculated through Eq. (24):

$$\nu_3 = 2k_3[(\mathrm{Ru^{IV}})][\mathrm{ROH}] \quad (24)$$

Using Eq. (15) to express $[(\mathrm{Ru^{IV}})]$ in terms of $[\mathrm{Ru}]_T$ gives Eq. (25):

$$\nu_3 = 2k_3[\mathrm{ROH}]\left(\frac{k_{-1}[\mathrm{HO}^-] + k_2[\mathrm{ROH}]}{k_1 + k_{-1}[\mathrm{HO}^-] + k_2[\mathrm{ROH}]}\right)[\mathrm{Ru}]_T \quad (25)$$

This expression can be simplified using $k_1 \ll k_{-1}[\mathrm{HO}^-]$ (which applies to 2-propanol and benzyl alcohol) to give Eq. (26):

$$\nu_3 = 2k_3[\mathrm{ROH}]\left(\frac{k_{-1}[\mathrm{HO}^-] + k_2[\mathrm{ROH}]}{k_{-1}[\mathrm{HO}^-] + k_2[\mathrm{ROH}]}\right)[\mathrm{Ru}]_T = 2k_3[\mathrm{ROH}][\mathrm{Ru}]_T \quad (26)$$

This expression is equivalent to Eq. (20) for b_1. Under the conditions in Figure 5 with 0.050 M NaOH (a typical value), ν_3 represents 18% of the observed rate. As expected, alcohol oxidation by the protonated form of the catalyst, $\mathrm{H(Ru^{IV})^+}$, is largely responsible for the observed rate. The moderate kinetic deuterium isotope effect ($\nu_{obs,H}/\nu_{obs,D} = 4.9$) would largely represent k_2 and indicate that this step likely involves the cleavage of an alcohol C–H bond.

For benzyl alcohol oxidation, the following expressions for c_1, c_2, and c_3 make Eq. (23) fit the observed behavior represented by Eq. (5):

$$c_1 = \frac{2k_1k_2[\mathrm{ROH}][\mathrm{Ru}]_T}{k_{-1}} \quad (27)$$

$$c_2 = \frac{2k_{-1}k_3[\mathrm{ROH}][\mathrm{Ru}]_T}{k_{-1}} = 2k_3[\mathrm{ROH}][\mathrm{Ru}]_T \quad (28)$$

$$c_3 = \frac{k_2[\mathrm{ROH}]}{k_{-1}} \quad (29)$$

Table IV lists values of k_1, k_3, k_2/k_{-1}, and ν_3/ν_{obs} obtained from Eqs. (27), (28), (29), and (26) for benzyl alcohol, 4-nitrobenzyl alcohol, and 4-methoxybenzyl alcohol. The values for k_1 are within experimental error of each other as would be expected for this mechanism. The results for ν_3/ν_{obs} confirm that alcohol oxidation by the protonated catalyst, $\mathrm{H(Ru^{IV})^+}$, is the major contributor to the observed oxidation chemistry.

Table IV Rate Constants from Eq. (23) for the Oxidation of Benzyl Alcohols[a]

Substrate	k_1 ($\mathrm{s^{-1}}$)	k_3 ($\mathrm{M^{-1}\ s^{-1}}$)	k_2/k_{-1} ($\mathrm{M^{-1}}$)	ν_3/ν_{obs}
4-Methoxybenzyl alcohol	$(4.5 \pm 0.8) \cdot 10^{-2}$	5.3 ± 0.4	44 ± 8	0.19 ± 0.03
Benzyl alcohol	$(4.4 \pm 2.4) \cdot 10^{-2}$	5.1 ± 0.9	40 ± 19.8	0.20 ± 0.06
4-Nitrobenzyl alcohol	$(5.7 \pm 1.7) \cdot 10^{-2}$	13.4 ± 1.7	82 ± 21	0.26 ± 0.03

[a] Reactions carried out with $[\mathrm{Ru}]_T = 1.00 \cdot 10^{-4}$ M; $[\mathrm{K_3Fe(CN)_6}] = 1.7 \cdot 10^{-3}$ M; [Alc.] $= 6.7 \cdot 10^{-4}$ M, $\mu = 0.50$ M at 25°C. ($\mathrm{NaClO_4}$ added to adjust ionic strength to 0.50 M.)

The moderate isotope effect for the oxidation of benzyl alcohol ($\nu_{obs,H}/\nu_{obs,D} = 4.2$) clearly represents a primary kinetic deuterium isotope effect in k_2 indicating cleavage of an alcohol C—H bond in this step.

Values for k_2/k_{-1} and k_3 show electron-withdrawing and -releasing substituents accelerating both k_2 and k_3 over their values for unsubstituted benzyl alcohol. This is consistent with the unusual concave shape of the attempted Hammett plot for 4-substituted benzyl alcohols (Fig. 7). Since the kinetic behavior of both 4-methoxybenzyl and 4-nitrobenzyl alcohols mirror that of benzyl alcohol, these substituent effects may represent shifts in the transition states of k_2 and k_3 [26]. Increases in k_2 and k_3 with electron-withdrawing and -releasing substituents suggest the buildup of modest negative and positive charges, respectively, at the alcohol carbon in the reaction with both protonated and unprotonated forms of the catalyst. Although the formation of radical intermediates could account for such behavior, this system exhibits no ring opening in the oxidation of cyclopropyl methanol and cyclobutanol radical-clock substrates and exhibits no oxygen dependence. A more consistent explanation for the substituent effects is a concerted mechanism in which alcohol deprotonation accompanies hydride transfer from an alcohol C—H bond to an oxo ligand. The partial charge that accumulates on the alcohol carbon would depend on the relative timing of these two events; electron-withdrawing substituents would encourage more alcohol deprotonation and more negative charge buildup in the transition state. The solvent isotope effects for 4-nitrobenzyl alcohol [$\nu_{obs}(H_2O)/\nu_{obs}(D_2O) = 1.88$] and 4-methoxybenzyl alcohol [$\nu_{obs}(H_2O)/\nu_{obs}(D_2O) = 1.63$] appear consistent with the expectation for greater O–(H,D) cleavage in the oxidation of 4-nitrobenzyl alcohol. Since the hydroxide dependence in the kinetics precludes attack of solution hydroxide in k_2 or k_3, the catalyst may be responsible for both C—H and O—H cleavage as part of a pericyclic process (Scheme I). Overall, this would amount to a two-electron–two-proton reduction of the catalyst, which is not surprising in light of the familiar proton-coupled electrochemistry of ruthenium-aquo/hydroxyl/oxo complexes [16,17].

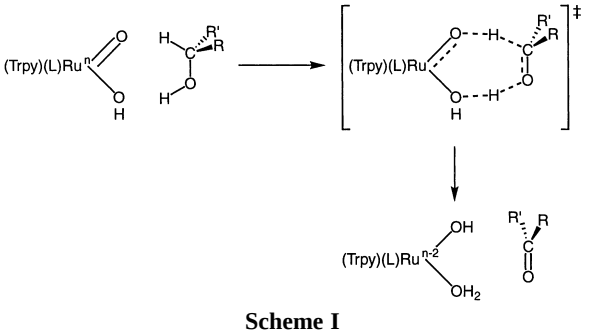

Scheme I

Although pericyclic mechanisms have been proposed for the oxidation of coordinated alcohols in chromium(VI)-, rhenium(V)-, and ruthenium(VI)-oxo complexes, this system provides evidence for a possible pericyclic oxidation of an uncoordinated alcohol [27–33]. In nonaqueous media, terpyridine ruthenium-oxo complexes oxidize alcohols by simple hydride-transfer. The strong alkaline environment in this system may support a low protonation state of the ruthenium catalyst that can act as a base as well as a hydride acceptor. Simultaneous alcohol deprotonation and hydride transfer would avoid energetic carbocation and radical intermediates and may exhibit activation enthalpies significantly below that of hydride transfer alone. This may make catalytic alcohol oxidation possible at low oxidation potentials. Although this issue is not so important for synthesis, it is particularly important for direct alcohol fuel cells in which the anode needs to collect electrons from alcohols near their thermodynamic oxidation potentials. A detailed survey of the substituent effects on k_2 and k_3 and their activation parameters is underway.

The authors acknowledge the financial assistance of the Camille and Henry Dreyfus Foundation and the donors of the Petroleum Research Fund administered by the American Chemical Society. We would also like to thank the Office of Graduate Programs and the College of Science and Mathematics at California State University, Northridge.

BIBLIOGRAPHY

1. Griffith, W. P. Chem Soc Rev 1992, 179.
2. Mucientes, A. E.; Poblete, F. J.; Rodriguez, D.; Rodriguez, M. A.; Santiago, F. Int J Chem Kinet 1999, 31(1), 1.
3. Behari, K.; Narayan, H.; Shukla, R. S.; Gupta, K. C. Int J Chem Kinet 1984, 16, 195.
4. Dwivedi, R. K.; Verma, K. M.; Kumar, P.; Behari, K. Tetrahedron 1983, 39(5), 815.
5. Lalitha, T. V.; Rao, M. P.; Sethuram, B. Indian J Chem 1992, 31A, 309.
6. Navarro, M.; De Giovani, W. F.; Romero, J. R. Synth Commun 1990, 20(3), 399.
7. Navarro, M.; Galembeck, S. E.; Romero, J. R.; De Giovani, W. F. Polyhedron 1996, 15(9), 1531.
8. Meyer, T. J. J Electrochem Soc 1984, 131, 221C and references therein.

9. Sullivan, B. P.; Calvert, J. M.; Meyer, T. J. Inorg Chem 1980, 19, 1404.
10. Wilberg, K. B.; Stewert, R. J Am Chem Soc 1955, 77, 1786.
11. Freeman, F.; Brant, J. B.; Hester, N. B.; Kamego, A. A.; Kasner, M. L.; McLaughlin, T. G.; Paull, E. W. J Org Chem 1970, 35(4), 982.
12. Maillard, B.; Forest, D.; Ingold, K. U. J Am Chem Soc 1976, 98, 7024.
13. Effio, A.; Griller, D.; Ingold, K. U.; Beckwith, A. L. J.; Serelis, A. K. J Am Chem Soc 1976, 102, 1734.
14. Attempts to isolate the catalytic intermediate including concentration and counterion precipitation techniques resulted in obvious spectroscopic changes and poorly defined products.
15. Roecker, L.; Kutner, W.; Gilbert, J. A.; Simmons, M.; Murrya, R. W.; Meyer, T. J. Inorg Chem 1985, 24, 3784.
16. Dobson, J. C.; Meyer, T. J. Inorg Chem 1988, 27, 3283.
17. Adeyemi, S. A.; Dovletglou, A.; Guadalupe, A. R.; Meyer, T. J. Inorg Chem 1992, 31, 1375.
18. Lebeau, E. L.; Adeyemi, S. A.; Meyer, T. J. Inorg Chem 1998, 37, 6476.
19. Dovletglou, A.; Meyer, T. J. J Am Chem Soc 1994, 116, 215.
20. Cheng, S. Y. S.; James, B. R. J Mol Catal 1997, 117, 91.
21. Tokita, Y.; Yamguchi, K.; Watanabe, Y.; Morichima, I. Inorg Chem 1993, 32, 329.
22. Moyer, B. A.; Sipe, B. K.; Meyer, T. J. Inorg Chem 1981, 20, 1475.
23. Thompson, M. S.; Meyer, T. J. J Am Chem Soc 1982, 104, 4106.
24. Lee, D. G.; van den Engh, M. Can J Chem 1972, 50, 200.
25. Dovletoglou, A.; Meyer, T. J. J Am Chem Soc 1994, 116(1), 215.
26. Swain, C. G.; Langsdorf (Jr), W. P. J Am Chem Soc 73, 1951, 2813.
27. Wang, Z.; Chandler, W. D.; Lee, D. G. Can J Chem 1998, 76, 919.
28. Deng, L.; Ziegler, T. Organometallics 1997, 16, 716.
29. Dumez, D. D.; Mayer, J. M. Inorg Chem 1995, 34, 6396.
30. Scott, S. L.; Bakac, A.; Espenson, J. H. J Am Chem Soc 1992, 114, 4205.
31. Rocek, J.; Westheimer, F. H.; Eschenmoser, A.; Moldovanyi, L.; Schreiber, J. Helv Chim Acta 1962, 45, 2554.
32. Wilberg, K. B.; Schafer, H. J Am Chem Soc 1967, 89, 455.
33. Lee, D. G.; Stewart, R. J Org Chem 1967, 32, 2868.